Land use classification of small agricultural parcels using multiple synthetic aperture radar images

Takanori Nagano
Graduate School of Agricultural Science
Kobe University
Kobe, Japan
naganot@ruby.kobe-u.ac.jp

Yoichi Fujihara
Graduate School of Bioresources and Environmental Sciences
Ishikawa Prefectural University,
Kanazawa, Japan

Abudukeremu Ainalibanua
Graduate School of Agricultural Science
Kobe University
Kobe, Japan

Natsuki Yoshikwa
Faculty of Agriculture
Niigata University
Niigata, Japan

***Abstract*—The aim of this research is to develop a robust and cost-effective methodology to monitor agricultural land use on a broad scale. Two different types of Synthetic Aperture Radar (SAR) images were compared to identify agricultural land use of small parcels in the middle and mountainous parts of Japan. Three study sites in Japan were chosen, with different geography and crop calendar. Main land use such as paddies, soybean fields and abandoned fields were assessed for their temporal backscattering coefficient (BC) change. It was relatively easier to identify paddies from other land use due to the sharp decrease in BC during the ponding period, typically between DOY (day of year) 130 and 170. Paddies and non-paddies were identified with Sentinel-1 single polarization VV data with a ground spatial resolution of 5×20 m down to parcels of 10-15 a when 5 images during the possible ponding periods were used for decision-tree classifications. Alos-2 spotlight mode 1 (single polarization HH) with a spatial resolution of 3×3 m exhibited a higher accuracy in the same identification, using only three images. Identification was possible down to parcels of 5-10 a. Ponding conditions however could not provide accurate enough identification for practical use. For soybean and abandoned fields, there was no clear signature to distinguish between the two since the state of the abandoned fields varied significantly.**

Keywords— Remote sensing, SAR, Midori-net, abandoned field, paddy

I. INTRODUCTION

The agricultural land use in Japan is now facing a critical change. Aging of farmers and depopulation in rural areas are causing severe workforce shortage. The profit margin of rice is becoming marginal as the increasing import and declining domestic consumption dampen the market price. It is thought that the abandoned agricultural parcels amounting to 420,000 ha in 2015, would rise further in the coming years (MAFF, 2015 [1]). Under such circumstances, it is increasingly important to monitor the dynamics of agricultural land use frequently enough to prepare countermeasures. However in Japan, agricultural land use survey is carried out at national scale only once in every 5 years based on questionnaires (MAFF, 2015 [2]).

Countries like USA and Canada produce national crop maps every year using remote sensing (e.g. USDA, 2018 [3]). Typically, mid-resolution imageries like Landsat are used for such purposes. There are many technical and financial challenges to carry out similar missions in Japan. First Japanese agricultural parcels are small, typically less than 30 a (3,000 m2) which cannot be correctly captured with mid-resolution imageries. High-resolution images however are too costly to cover a large area. Second, the main agricultural season in Japan is March through to November with many cloudy and rainy days in summer due to monsoon. This limits the availability of cloud-free optical images. Third, signature detection of crops is difficult as the climate and crop calendar vary by region.

The purpose of this study is to develop a robust and cost-effective methodology for agricultural land use classifications on a broad scale in Japan. We focus on using mid-resolution satellite images which have recently been made available to the public for access. Synthetic aperture radar (SAR) images have proven effective in crop land detection in Japan because of regular data availability, unaffected by clouds. Takeuchi et al. (2000) [4] compared C-band and L-band SAR for crop land classifications including paddies and concluded that C-band SAR images have an advantage over L-band SAR which is often affected by Bragg Scattering. They also reported that paddy can be detected by detecting a decline of backscattering coefficient (BC) with ponding in paddies. Mukai et al. (2002) [5] proposed a combined use of SAR and optical images to increase signature for more accurate paddy detection. Takahashi et al. (2003) [6] proposed use of parcel outline data for object-based classification. For ASTER data with a spatial resolution of 15 m, they reported an increase of accuracy by 9%. Land use identification at parcel scale was proposed by

Suzuki et al. (2009) [7] with a combined use of high-resolution SAR imageries (COSMO-SkyMed) and parcel outline data.

Table 1. Land uses and areas of agricultural parcels in 3 different study sites in Japan

		Sasyama		Yoshikawa		Yabu	
		Parcels	Percentage	Parcels	Percentage	Parcels	Percentage
Land use	Paddy	1,063	62%	1,916	67%	1,369	47%
	Soybean	409	24%	167	6%	5	0%
	Abandoned	123	7%	550	19%	1,012	35%
	Other	126	7%	223	8%	524	18%
	Total	**1,721**		**2,856**		**2,910**	
Area	0-5a	220	13%	442	15%	1,194	41%
	5-10a	293	17%	502	18%	719	25%
	10-15a	305	18%	431	15%	444	15%
	15-25a	457	27%	715	25%	353	12%
	25-80a	446	26%	766	27%	200	7%

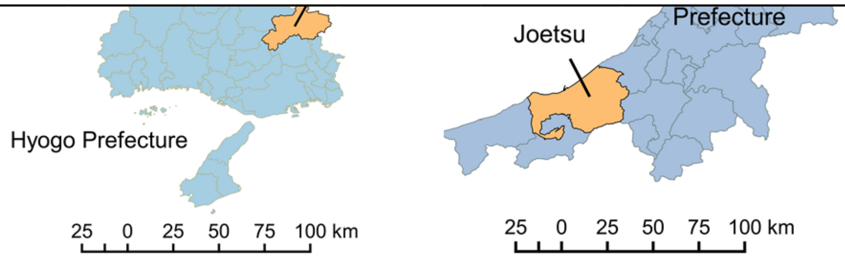

Figure 1. Study Areas

Osawa et al. (2010) [8] proposed use of time-series ASTER data and sequential classification for more accurate parcel land use detection. In 2011, parcel outline data became available on Midorinet, a union of land improvement districts in each prefecture of Japan [9].

We aim to classify three important land uses in a country that are rice, soybean and abandoned fields. We started the study in 2016 using time-series C-band SAR and regularly available and accessible Sentinel-1 images. Parcel outline data from Midorinet was used to raise accuracy of the classification. The classification had a fair accuracy for parcels larger than 16 a, but not for smaller parcels (Nagano et al., 2017) [10]. Therefore, in this study we used L-band SAR, Alos-2 in addition and compared accuracy.

II. MATERIALS AND METHODS

A. Study Area

Agricultural land use survey was carried out visually in September 2016, using aerial photos taken by a drone in two different locations. Sasayama city, Hyogo Prefecture (hereafter referred to as "Sasayama"), is situated on a plateau (altitude: 205 m). Farms are spread along rivers, sometimes reaching to the foot of mountains. Yoshikawa Land Improvement District in Joetsu, Niigata Prefecture (hereafter referred to as "Yoshikawa") is situated not far from the coast of the Sea of Japan. The district stretches from the coastal plain to the narrow valleys in mountains. In September 2017, Yabu city, Hyogo Prefecture, was added to the two study areas above (hereafter referred as "Yabu"). It is a mountainous region with small agricultural parcels situated along rivers, sometimes terraced on the hills. The main land use in Sasayama and Yoshikawa are rice soybean and abandoned fields. In Yabu, rice, abandoned fields and vegetable fields are three major land uses. There are many abandoned fields in Yabu because the parcel size is very small. The locations and characteristics of the three areas are shown in Figure 1 and Table 1.

B. Data

In this study, C-band SAR, Sentinel-1 images (European Space Agency) with a ground spatial resolution of 5×20 m (single polarization VV) and L-band SAR, Alos-2 (JAXA) images with a spatial resolution of 3×3 m (mode SM1, single polarization HH) were used for comparison. Sentinel-1 has a revisit time of 12 days (6 days since 2017 due to the constellation) and Alos-2 14 days. For Alos-2, observations are performed in various modes, therefore there is a much longer interval than 14 days in between image acquisitions in the same mode. Analysis

C. Analysis

For SAR images, raw images were preprocessed (geometrically corrected with Alos AW3D30 (JAXA) as the DEM and geocoded) using ENVI Sarscape (Harris Geospatial) Ver. 5.4. Refined Lee filtering was applied once before geocoding. Obtained images with backscattering coefficients (BC) were superimposed on the agricultural parcel vector data of each area, Midorinet, and the representative value of each parcel was obtained using ArcGIS (ESRI).

For classification, decision-tree library (rpart) of the statistical software (R) was used to determine threshold values of BC. Kappa coefficient (κ) were calculated to evaluate the accuracy of classification.

$$\kappa = \frac{p_0 - P_e}{1 - P_e} \quad (1)$$

where p_o: the relative observed agreement among raters, p_e: the hypothetical probability of chance agreement, using the observed data to calculate the probabilities of each observer randomly seeing each category.

III. RESULTS AND DISCUSSIONS

A. Backward scattering coefficient signature of paddy

Figure 2 and 3 show temporal change of BC from Sasayama's paddies of different sizes detected by Sentinel-1 and Alos-2 in 2016. For Sentinel-1, BC takes value of -8 to -10 dB in the field raising period (around 100 cumulative days from January 1). When ponding initiated BC decreased by about 5 dB because of smoother surface of ponded water. The extent of this decrease differs according to the size of parcels. This is probably due to mixed land use occurring in pixels as target parcels get smaller. For Alos-2, a similar decrease in BC from ponding was observed. The difference due to parcel size also occurred despite of finer resolution of the imagery. For L-band, the radar wave reflected on water surface can scatter at different locations (e.g. ridges and surrounding forests) and contribute to backscatter. The sharp contrast in the ponding and non-ponding period was not observed in Yoshikawa in the early spring. L-band seems to be more sensitive to soil moisture and BC tends to be small even when paddy is not ponded.

B. Backward scattering coefficient signature of soybean

Figure 4 and 5 show temporal change of BC for soybean in Sasayama observed by Sentinel-1 and Alos-2 respectively in 2016. For Sentinel-1 BC dropped from DOY 100 to DOY 125 then increased toward DOY 200. Even on agricultural parcels of 5-10a, signatures similar to larger agricultural parcels were detected (Figure 5). With Alos-2, BC reached the lowest value at DOY 150 and then gradually increased to the maximum value obtained at around DOY 270 (Figure 6). The signatures of smaller parcels were relatively well captured. DOY 150 happens to be a transplanting period of seedlings and thus soil is tilled, furrowed and bare. DOY 270 is the harvesting period. L-band SAR seems to capture biomass increase on the ground. The difference caused by parcel size is attributed to loss of land-use-specific signature as parcel size gets smaller and occurrence of mixed cells increases.

C. Backward scattering coefficient signatures of abandoned fields

Figure 6 shows a comparison of BC from soybean and abandoned fields for Sasayama and Yoshikawa observed by Sentinel-1. BC of the abandoned field showed a similar signature to soybean, and there was no obvious signature to distinguish one from the other. The obvious difference between Sasayama and Yoshikawa was the low tendency of BC in the early spring in Yoshikawa due to snow coverage. For abandoned fields, the level of weed growth and management varies (some fields near households are mowed or tilled once a year whereas others are left untouched) thus it is difficult to distinguish abandoned fields from soy or other land usages with simple rules.

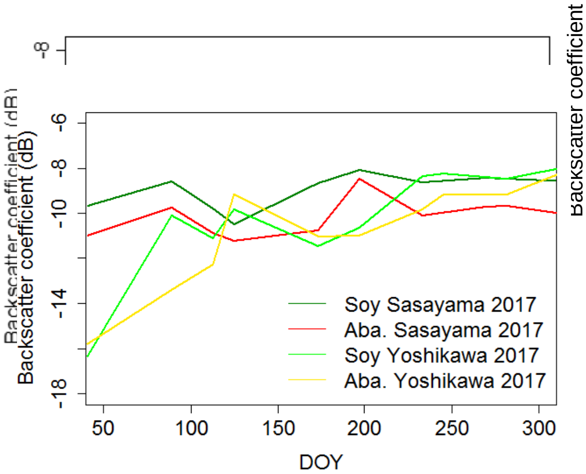

Figure 6. Backscatter coefficients of soybean and abandoned fields observed by Sentinel-1in Sasayama, 2016.

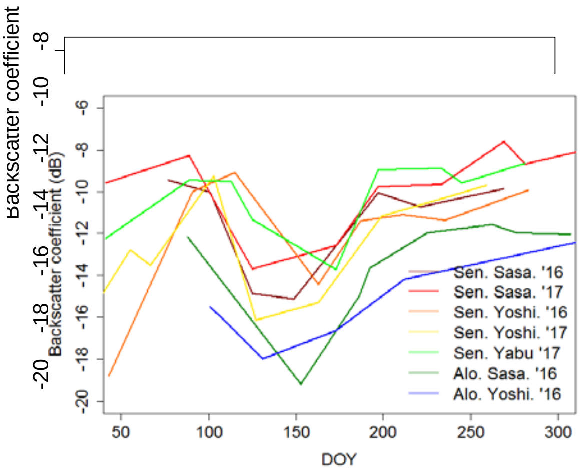

Figure 7. Backscatter coefficients of soybean and abandoned fields observed by Sentinel-1in Sasayama, 2016.

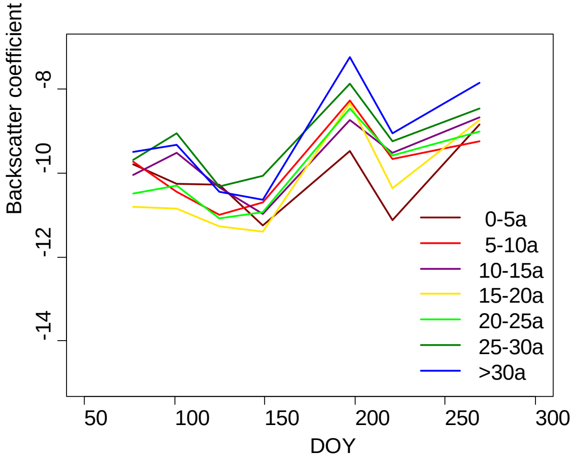

Figure 4. Backscatter coefficients of soybean fields observed by Sentinel-1in Sasayama, 2016.

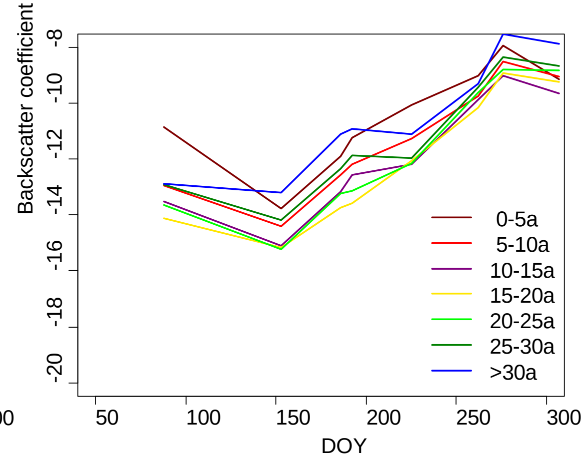

Figure 5. Backscatter coefficients of soybean fields observed by Alos-2 in Sasayama, 2016.

D. Appropriate period for paddy detection

From the results above, it seems reasonable to detect paddy fields first among different land use. Figure 7 shows a BC change of paddy fields at different sites detected by two different SAR images. Even among different sites, it is highly probable that paddy fields have ponded water between DOY 130 and DOY 170. Therefore, images available within this period are most eligible for accurate paddy detection.

E. Accuracy of paddy detection

Table 2Images used for paddy and non-paddy classification

Sensor	Site	Day of image acquisition in 2017	
Sentinel-1	Sasayama	May 5, May 17, May 29, June 10, June 22	
	Yabu	May 5, May 17, May 29, June 10, June 22	
	Yoshikawa	May 7, May 19, May 31, June 12, June 24	
Alos-2	Sasayama	March 13, May 17, June 19	
	Yabu	Feb 27, Apr. 24, June 5	
	Yoshikawa	Mar. 17, June 20 (only 2 data were available)	

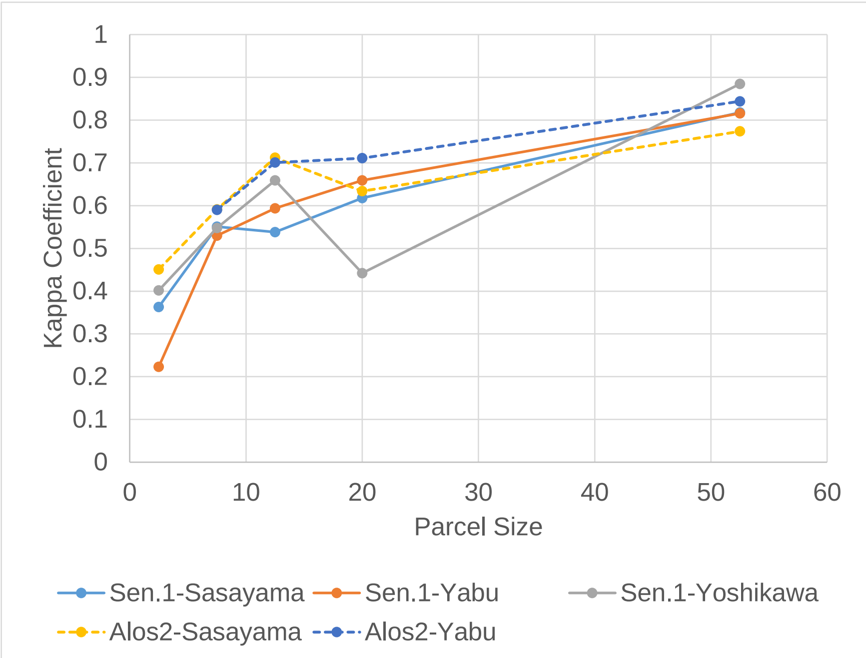

Figure 8. Comparison of reproducibility of classification ofpaddy and non-paddy in 2017

Figure 8 shows a comparison of reproducibility of paddy and non-paddy classifications. For Sentinel-1, 5 images from late April to late June with 12-day intervals were used. The decision-tree algorithm picked the best 3 thresholds which are statically significant from these dates. For Alos-2, images were much less available and 3 images available for each study site between late February and late June were all fed to decision-tree classification (For Yoshikawa classification was not possible due to availability of only two images). Table 2 shows the images used for classification at each site. Thresholds vary according to the grouping of parcel size, namely 0-5a, 5-10a, 10-15a, 15-25a and 25-80a. This means that they can be the best value for reducibility of classification of any single group.For 25-80a, both Sentinel-1 and Alos-2 offer κ around 0.8 which is considered excellent for classification. In this case, it was equivalent to a total accuracy of more than 0.9. For 15-25a, κ is between 0.6 and 0.7 but for Yoshikawa with Sentinel-1. κ is low in Yoshikawa as non-paddy fields accounted for only 4.6% of 715 parcels. Value of κ between 0.6 and 0.8 is considered good but not reliable enough for operational use. As parcel size gets smaller than 15 a, Alos-2 results in better classification although not all images capture ponding period. With Alos-2, parcels between 5 and 10 a are classified with κ close to 0.6. These higher accuracies are attributed to the finer resolution of the imagery. However, for fields between 0 and 5 a classification is no longer reliable even with Alos-2. Alos-2 isexpected to exhibit better classification accuracy if more images are available between DOY 130 and DOY 170. For Sentinel-1 classification down to 15 a seems to be the limit in terms of reliability.

These results revealed that paddy detection solely relying on detection of ponding is effective but not accurate enough for operational use. This is reasonable since ponding could occur in non-paddy fields after heavy rainfall or due to water logging in the low-lying area and some paddies run dry due to erratic water management. Signature addition from BC later in the season or NDVI [5],[6] seems necessary.

IV. CONCLUSION

Temporal images captured with C-band and L-band SAR were compared to identify rice, soybean and abandoned fields at parcel level. Sentinel-1 single polarization VV data with a ground spatial resolution of 5×20 m identified paddies and non-paddies down to parcel size of 15 a with Kappa coefficient of more than 0.6 when 5 images during the possible ponding period were used for decision-tree classifications. Alos-2 spotlight mode 1 (single polarization HH) with a spatial resolution of 3×3 m performed identification down to parcel size of 5a. For soybean and abandoned fields, there was no clear signature to distinguish between the two possibly because there was a large variation in the state of abandoned fields.

ACKNOWLEDGMENT

This research was carried out under Grant-in-Aid No. 16K 07942 and JAXA 1st Earth Observation Research Announcement (RA 1 R 701). Midori-net provided us parcel vector data.

REFERENCES

[1] Ministry of Agriculture, Forestry and Fisheries, Kouhainouchi no genjou to taisaku ni tsuite (The state of devastated agricultural land and countermeasures), http://www.maff.go.jp/j/nousin/tikei/houkiti/pdf/2804_genjo.pdf, last viewed on Sep. 8, 2018, (2015).

[2] Ministry of Agriculture, Forestry and Fisheries, Census, http://www.maff.go.jp/e/data/stat/index.html, last viewed on Oct. 22, 2018, (2015).

[3] USDA National Agricultural Statistic Service, CropScape, https://nassgeodata.gmu.edu/CropScape/, last viewed on Aug. 29, 2018 (2018).

[4] Takeuchi S., Konishi T., Suga Y. and Oguro Y., Rice planted area estimation in early stage using Space-borne SAR data, Journal of the Japan Society of Photogrammetry, 39 (4), (2000), pp 25-30.

[5] Mukai Y., Rikimaru A., Takahashi K. and Sugawara, K., Estimation of rice acreage by satellite borne Synthetic Aperture Radar and optical sensor data, Technical report of the Technological University of Nagaoka, Vol. 24, (2002), pp 23-28.

[6] Takahashi K., Rikimaru A. and Mukai Y., Verification of high precise estimation method of the rice planted fields acreage with outline data reference using ASTER/VNIR Image, Journal of the Japan Society of Photogrammetry, Vol. 42, No. 4, (2003), pp 18-26.

[7] Suzuki K. and Shibata J., Detection of rice planted plots using COSMO-SkyMed imageries. Journal of the Japanese Agricultural Systems Society, Vol. 25, No. 4, (2009), pp 215-220.

[8] Osawa K., Kunii D. and Saito G., Classification of arable land using multi-temporal Terra/ASTER data. Journal of the Japanese Agricultural Systems Society, Vol. 26, No. 2, (2010), pp 67-77.

[9] Midorinet, National federation of Land Improvement districts, http://www.inakajin.or.jp/jigyou/tabid/185/Default.aspx, last viewed on 31 Aug. 2018, (2014).

[10] Nagano T., Asano T., Kotera A., Fujihara Y. and Yoshikawa, N., Plot-by-plot classification of agricultural land use by mid-resolution satellite imageries, proceedings of annual meeting of JSIDRE (2017).